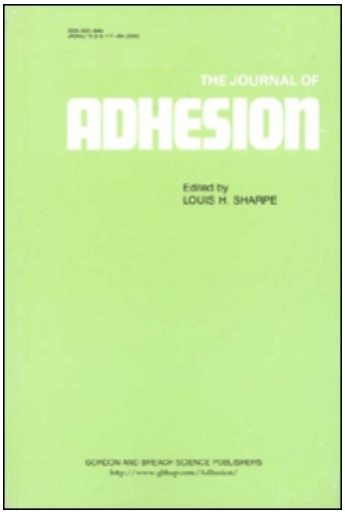

The Journal of Adhesion
Publication details, including instructions for authors and subscription information:
http://www.informaworld.com/smpp/title~content=t713453635

The Characterization of the Energy of Fracture at or near Interfaces Between Viscoelastic Solids

John M. Bowen[a]; Wolfgang G. Knauss[b]
[a] Jet Propulsion Laboratory, Pasadena, California, U.S.A. [b] Graduate Aeronautical Laboratories, California Institute of Technology, Pasadena, California, U.S.A.

To cite this Article Bowen, John M. and Knauss, Wolfgang G.(1992) 'The Characterization of the Energy of Fracture at or near Interfaces Between Viscoelastic Solids', The Journal of Adhesion, 39: 1, 43 — 59
To link to this Article: DOI: 10.1080/00218469208026537
URL: http://dx.doi.org/10.1080/00218469208026537

J. Adhesion, 1992, Vol. 39, pp. 43–59
Reprints available directly from the publisher
Photocopying permitted by license only

Printed in Great Britain

The Characterization of the Energy of Fracture at or near Interfaces Between Viscoelastic Solids*

JOHN M. BOWEN

Jet Propulsion Laboratory, Pasadena, California, U.S.A.

WOLFGANG G. KNAUSS**

Graduate Aeronautical Laboratories, California Institute of Technology, Pasadena, California 91125, U.S.A.

(Received January 28, 1992; in final form May 20, 1992)

The problem of separating two viscoelastic solids of different properties in a time dependent manner is considered. This work is part of a wider study concerned with the time dependent failure of viscoelastic adhesive bonds at and/or near the interface, including propagation of a crack away from the interface. Inasmuch as such a study requires sufficient bond strength to control the orientation of crack propagation, this paper deals with the characterization of interface strength. Following earlier analysis of crack propagation in homogeneous and bimaterial viscoelastic solids, experimental studies concerned with rate dependent fracture at the interface are evaluated in terms of the viscoelastic functions associated with homogeneous fracture of the adherends and a separate interface-intrinsic strength which is determined by the chemistry at the interface. This interface strength multiplies a viscoelastic function, which, for the interface problem, is a combination of the properties of the homogeneous solids. Interface strength on the same order as those of the adherends is achieved.

KEY WORDS Bimaterial interface; interface crack; time-dependent failure; viscoelastic adhesive bonding; failure strength/interface strength.

1 INTRODUCTION

Joining materials of different physical properties has been an engineering practice of extreme importance ever since man learned to make tools for survival. While early man relied to a large degree on natural adhesives to join components of bows and arrows, the increasing use of metals, especially with the rise of the industrial revolution, favored mechanical fasteners to exploit the high strength of the joined components. However, today's advances in development of strong polymeric adhesives makes it possible to consider and achieve strong bonds between materials of

*Presented at the 14th Annual Meeting of The Adhesion Society, Inc., Clearwater, Florida, U.S.A., February 17–20, 1991.

**Corresponding author.

widely different properties. A special class of these construction materials comprises the polymers themselves, as exemplified in the development of aerospace and automotive composite materials and steel-rubber joining in tires and shock isolation supports; equally noteworthy are developments in polymer-to-polymer bonds in polymers reinforced with polymer fibers and adhesive joining in such diverse applications as solid propellant rocket motors and automobile tires.

In dealing with the design strength or the evaluation of such bond strengths the recurring question arises as to how the bond strength is to be characterized. In some situations the peel test provides a numerical basis for qualitative comparison, in spite of the fact that this test rarely provides firm data for bond design in situations where the peel geometry, with its involvement of large deformation flexing of at least one of its members, is not duplicated closely. In this paper we address the determination and interpretation of interfacial failure strength in energy terms with the intention of defining a fractional strength of an optimal value. This proposition is made in the context of fracture mechanics for homogeneous linearly viscoelastic solids (small deformations) and draws on observations made in an earlier publication on the parallel between fracture in homogeneous solids and at interfaces.[1]

The motivation for the present work came, in part, from the need to generate optimal adhesive bonds between two polymers in order to investigate certain interfacial fracture phenomena connected with failure of either of the two adherends. The ability to cause fracture to propagate (to kink) away from the interface requires a "sufficiently high" bond strength, and this condition must prevail under load conditions which make such phenomena proceed with various speeds.

In studying this problem it seemed prudent to start with a material system which does not involve properties of materials which are widely diverse; that is, it was of interest to consider materials which have certain similarities, rather than be so different that any hope of understanding the system behavior in terms of known or expected failure response would be jeopardized. We look at this study, therefore, as an introduction to similar studies of wider scope, in which the results outlined below would be expanded and confirmed for systems of other material combinations. Also, inasmuch as the experimental materials used are elastomers, some nonlinear effects close to the crack tip are present. We ignore these more detailed deformation characteristics and limit the present analysis and interpretation to linear theory in the spirit of Reference 2.

In the sequel we review first the issues of time dependent failure at and near an interface, then proceed in section 3 to outline the manufacture of specimens which contain planar interfacial cracks and possess controllable interface "strength." The analytical modelling of these fracture specimens is presented in section 4. In section 5, the experimental procedure and the results of the tests are discussed along with the proposition of how to quantify the rate dependent bond strength for interfacial separation if the corresponding data for the two adherends are available.

2 REVIEW OF UNDERLYING ANALYTICAL DEVELOPMENTS

In earlier publications the relation of fracture progression has been established in terms of the rheological properties of homogeneous (linearly) viscoelastic solids,[2]

and an extension has been offered to apply these results to the time dependent interfacial separation process.[1] In this section we review first the salient issues of the monolithic fracture behavior of a viscoelastic solid and then the relation to interface separation. Making use of these results we then proceed to cast the separation problem in terms of behavior functions that can be associated with the time dependent fracture of each of the two joined materials, separately. In that process the definition of "the interface strength" will become clear in terms of an energy description.

2.1 Fracture of Monolithic, Viscoelastic Solids

The steady propagation of a crack in a homogeneous, (linearly) viscoelastic solid is governed by the relation[2] (locally in plane strain,[3] assuming a constant Poisson's ratio of $\nu = 1/2$)

$$2D^{\infty}\Theta(\alpha/c)K^2 = \frac{\Gamma}{1-\nu^2} \tag{1}$$

where D^{∞} is the long-term or equilibrium uniaxial creep compliance $\equiv 1/E^{\infty}$
K is the (current) stress intensity factor for the crack geometry considered
$\Theta(s)$ is a viscoelasticity function defined below
c is the speed of crack propagation
Γ is an intrinsic fracture energy (per unit crack advance) exhibited by the material in the limit of (near) zero crack speed, i.e. in the absence of viscoelastic effects, and
α is a length scale associated with the fracture process.

α may be a constant in some materials, but in a polyurethane similar to that studied here, it was found to make the experimental data fit equation (1) excellently if it was identified with the Dugdale/Barenblatt parameter

$$\alpha \equiv \frac{\pi K^2}{8\sigma_o^2} \tag{2}$$

in which σ_0 denotes the ultimate cohesive stress of the solid.

The function $\Theta(s)$ is defined in terms of the uniaxial creep compliance $D(t) = D_0 + \Delta D(t)$, $D_0 = const. = D(0)$, by

$$\Theta(s) = E^{\infty}\int_0^1 \left\{ D_0 F(\rho) - \int_{\rho}^1 \Delta D\left[s\cdot(r-\rho)\right]\frac{dF(r)}{dr}dr \right\} d\rho \tag{3}$$

where $F(r)$ is a non-dimensional function related to the crack tip stress field and deformation; this function is delineated in Reference 2.

The function $\Theta(s)$ is also well approximated by

$$\Theta(s) = \frac{1}{2}E^{\infty}D(s) \tag{4}$$

as shown in Reference 2 and implicit in the work of several investigators.[4–7] Accordingly, equation (1) may be written (approximately) as

$$D\left(\frac{\alpha}{c}\right)K^2=\frac{\Gamma}{1-\nu^2} \tag{5}$$

For completeness of presentation we note that this equation (as well as (1)) applies strictly in the case of constant crack speed, c, but applies also with good approximation to varying crack speeds, provided the condition

$$\frac{1}{K}\frac{\partial K}{\partial t}\ll\frac{c(t)}{2\alpha(t)} \tag{6}$$

is always met; in this case $K=K(t)$ is the time-varying stress intensity factor.[4,6]

In the sequel we continue to deal with the function

$$2\Theta\left(\frac{\alpha}{c}\right)\equiv\frac{1}{\Psi(\alpha/c)}, \tag{7}$$

which possesses the limit $2\Theta(\infty)=\dfrac{1}{\Psi(\infty)}=1$; Ψ is the time or velocity dependent component of the fracture energy determined in experiments, as shown later.

Equation (1) can then be written as

$$(1-\nu^2)D^{\infty}K^2=\frac{(1-\nu^2)K^2}{E^{\infty}}=\Gamma\cdot\Psi\left(\frac{\alpha}{c}\right) \tag{8}$$

and the stress intensity factor giving rise to different interface crack tip speeds, c, as

$$\mathrm{K}=\left[\frac{E^{\infty}\Gamma\Psi\left(\frac{\alpha}{c}\right)}{1-\nu^2}\right]^{1/2}. \tag{9}$$

One recognizes in the left hand side of (8) the combination of terms identified in linearly elastic fracture mechanics as the energy release rate for the solid in its globally relaxed state and the right hand side as the fracture energy, except that in the present case this energy depends on the speed of crack propagation; this combination of terms has been postulated before to represent a rate dependent fracture energy.[2,8] Moreover, one notes that the rate dependent fracture energy consists of a multiplicative operation of the time or rate (velocity) dependent function Ψ and the time-independent intrinsic fracture energy Γ.

2.2 Application to Interface Separation

It has been proposed[1] on the basis of equation (1) and on the analogy to elastic interface separation that fracture along an interface between viscoelastic materials is governed (approximately) by[9]

$$\left[D_1^{\infty}\Theta_1\left(\frac{\alpha}{c}\right)+D_2^{\infty}\Theta_2\left(\frac{\alpha}{c}\right)\right]K^2=\frac{\Gamma_i}{1-\nu^2} \tag{10}$$

where the constant Γ_i represents the intrinsic strength of the interface (intrinsic interface fracture energy) and Θ_1, Θ_2 are the viscoelastic functions of equation (3) for the two joined solids. Also, $K^2 = K_1^2 + K_2^2$ with K_1 and K_2 representing approximately the local mode I and II stress intensity factors. One notes that, because of equation (4), the factor in square brackets represents, with very good approximation, the average of the two compliances. In this formulation the length scale, α, is that scale appropriate for the debonding problem, but it is not clear at this time how that length scale is related to those appropriate for the two homogeneous materials by themselves. In fact, there is little hope at present that on the basis of linearly (visco)elastic fracture analysis such a general relation could be established analytically: Problems associated with the pathological behavior of the crack tip stress field seem to preclude such expectations.[10] In the interest of examining the simpler case alluded to in the Introduction we bypass further examination of that problem and assume that the size scales for the two solids studied here are sufficiently close so as not to pose a problem of first order: In effect, we are assuming then that the interface failure is governed approximately by the same size parameter as for the two materials separately. This expectation is based on the fact that we are dealing here with two polyurethanes, the molecular structures of which are not very different. It would be appropriate in a follow-on study to examine the consequences of a more distinctly different set of materials after one has learned how to control the interface strength of such a material combination.

We turn now to cast equation (10) in terms of functions and material parameters which describe the fracture of the homogeneous adherends. To that end we write

$$\frac{1}{2}(D_1^x + D_2^x)K^2 = \frac{\Gamma_i}{1-\nu^2}\left[\frac{D_1^x + D_2^x}{2D_1^x\Theta_1\left(\frac{\alpha}{c}\right) + 2D_2^x\Theta_2\left(\frac{\alpha}{c}\right)}\right] \tag{11}$$

$$= \frac{\Gamma_i}{1-\nu^2}\Psi_i\left(\frac{\alpha}{c}\right).$$

One notes in passing that this expression yields the elastic limit case in the event of vanishing crack speeds when the bracketed factor on the right hand side multiplying $\Gamma_i/(1-\nu^2)$ tends to unity. By analogy (*cf.* equation (8)) this bracketed expression is denoted by Ψ_i, the velocity dependent function appropriate to the interface itself. Thus the intrinsic fracture energy Γ_i characterizes the (minimum) strength of the interface simulating the situation for the fracture of a homogeneous solid. We believe this property of the interface to depend on its molecular structure, similar to the way in which the fracture energy of each of the homogeneous bodies depends on their molecular make-up.[11]

For completeness of presentation let us consider a special case, namely when one of the solids (say, solid "2") is rigid. In that event equation (11) reverts to

$$\frac{K^2}{E_1^x} = \frac{2\Gamma_i}{1-\nu^2}\frac{1}{2\Theta_1(\alpha/c)} = \frac{2\Gamma_i}{1-\nu^2}\Psi_1\left(\frac{\alpha}{c}\right) \tag{12}$$

which indicates that the time dependent failure of a polymer-rigid interface follows the same fracture law as that of a homogeneously viscoelastic solid (*cf.* equation

8)), except that the intrinsic fracture energy is replaced by twice the interface fracture energy in the separation case. One explanation for the factor of two is to observe that energy release is only provided by half of the solid which would make up the homogeneous problem. From a practical point of view the factor is often irrelevant, particularly in cases when Γ_i is not known separately from a series of independent fracture tests.

3 SPECIMEN PREPARATION

Bimaterial specimens were made of "Solithane 113," a polyurethane elastomer which serves as the model material in this study.[12] By varying the ratio of resin to curative, it is possible to cast homogeneous elastomers which encompass a considerable range of mechanical behavior.[13,14]. Of primary concern in this study of bimaterial interface fracture is the strength of the bond between the materials, and the integrity of what should ideally be a planar interface between them. We delineate here briefly the bimaterial specimen preparation technique described in Reference 15.

A bimaterial block, comprised of Solithane 55/45 and Solithane 45/55, is cast in two steps.[16] The 55/45 composition, henceforth referred to as "material 1" or the "hard" material, is prepared first: 308 grams of resin are added to 140 grams of virgin curing agent and 112 grams of dyed curing agent (0.1% dye by weight) in a 1000 ml Erlenmeyer flask.[17] The contents of the flask are mixed under vacuum for ten minutes at 65°C. Periodically throughout the mixing process, the vacuum is relaxed and nitrogen gas is briefly introduced in order to release O_2 and N_2 bubbles which develop inside the Solithane during the reaction.

The Solithane is transferred into a mold which has been maintained at 65°C and has been treated with a trichlorofluoroethane release agent[18] in order to facilitate the eventual removal of the cured sample. The mold is an aluminum parallelepiped with internal dimensions of 165 mm × 75 mm × 120 mm, the last dimension denoting its overall height.

The 55/45 material is heated to 80°C and held at this temperature until sufficient "gelling" has developed (about 40 minutes). This period is the most critical of the entire curing cycle because if the material is allowed to cure too much, subsequent chemical bonding across the interface is diminished, and the resulting interface will possess less than optimal (bond) strength. If, on the other hand, the curing process is not allowed to proceed far enough, the consistency of the 55/45 will be insufficient to prevent mixing or rippling upon the addition of the 45/55.

Once the 55/45 has attained the desired consistency, the mold is removed from the oven and maintained at room temperature. A thin sheet of Teflon (155 mm × 12 mm × 0.1 mm) is placed along and parallel to one of the longer edges of the free surface of the gelled 55/45. Then, 560 g of the 45/55 composition ("material 2") are prepared according to a procedure analogous to that used for the 55/45, with the exception of the use of dye. The 45/55 composition is introduced into the mold on top of the partially cured 55/45 and the Teflon sheet; the two compositions are then allowed to cure together. The Teflon provides an area of zero bond strength

located exactly at the interface between the two materials. It becomes the starter location from which to grow an interface crack.

The fully cured Solithane block is 165 mm × 75 mm × 80 mm, the last dimension denoting its height. The contrast in the colors of the two compositions clearly delineates the interface between them, and the transparency of the 45/55 layer permits observation of the internal Teflon strip.

Thin slices or sheets (~3 mm) are cut from the block with a saw and a specially-designed support apparatus which helps maintain specimen alignment. Approximately 30–35 specimens suitable for testing can be obtained from each block. To reduce the surface roughness introduced by the saw, the thin sheets are "polished" with wet sandpaper. The sheets are then coated with a fine layer of Solithane 40/60 which is allowed to cure overnight at 65°C. This coating, less than 0.1 mm thick, restores a smooth surface appearance to the specimens. Finally, thin aluminum loading grips are bonded to the specimen with an RTV silicone rubber adhesive, and holes required for specimen loading are provided in accordance with Figure 1.

Specimen preparation is completed by cutting the 5 mm ligament of Solithane behind the crack, which is defined by the Teflon strip. Finally, using the load frame described in a later section, the crack is forced to propagate along the interface for 2–3 mm so that a natural crack tip, located exactly at the interface, is obtained. This procedure eliminates the influence of the Teflon sheet on the ultimate geometry of the crack tip.

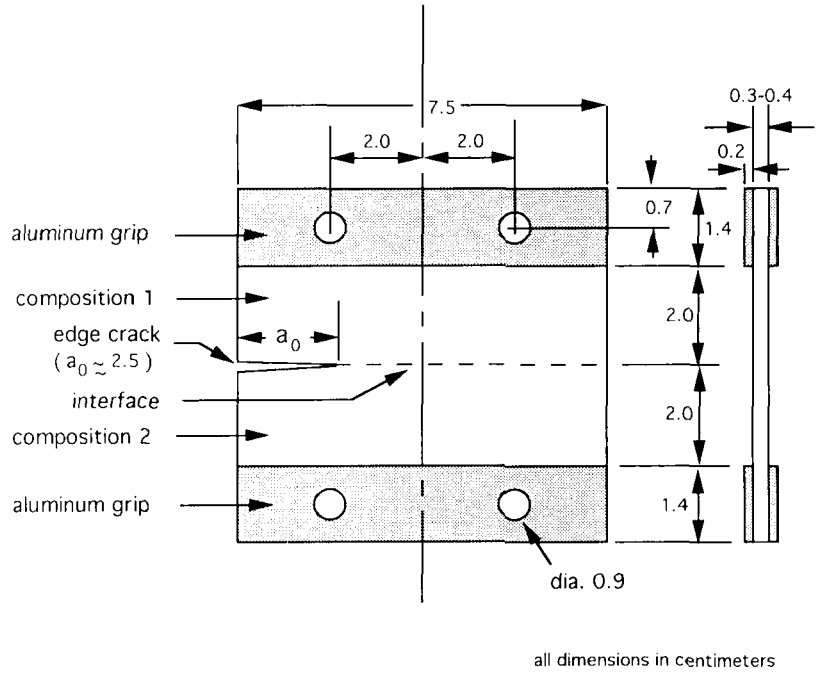

FIGURE 1 Geometry of the bimaterial specimen.

4 ANALYTICAL MODELLING OF THE FRACTURE SPECIMENS

In light of the equilibrium compliance of Solithane (at room temperature, $E^{\infty}_{55/45} = 3.19\,MPa$ and $E^{\infty}_{45/55} = 1.23\,MPa$), the aluminum grips ($E \approx 7 \times 10^4\,MPa$) bonded to its surface can be considered rigid (Figure 1). The nature of the highly constrained Solithane sandwiched between the grips on opposite faces of the specimen suggests that deformations within these regions can, to first order, be neglected. Thus the physical test specimen, subjected to applied displacements, U, as indicated in Figure 2, can be modelled by the simpler bimaterial system in which the displacements are applied uniformly along the lengthwise boundaries of the specimen.

Analysis of the crack tip stress field is accomplished numerically through finite element analysis using the code FEAP.[19] Details of that analysis are not presented here, and it suffices to state that the crack tip stress intensity factors are determined according to a plane stress, linearly elastic problem formulation.[20] In conjunction with this formulation, it must be noted that a reference length of 1 cm, representative of the unit of measure appropriate to this specimen geometry, is used implicitly in the determination of the interface stress intensity factors for the bimaterial case (this length parameter is absent from the homogeneous development).

If the applied displacements, U, are resolved into components u_1 and u_2 representing displacements parallel and perpendicular to the plane of the interface, they are given by

$$u_1 = U \sin\theta \text{ and } u_2 = U \cos\theta. \tag{13}$$

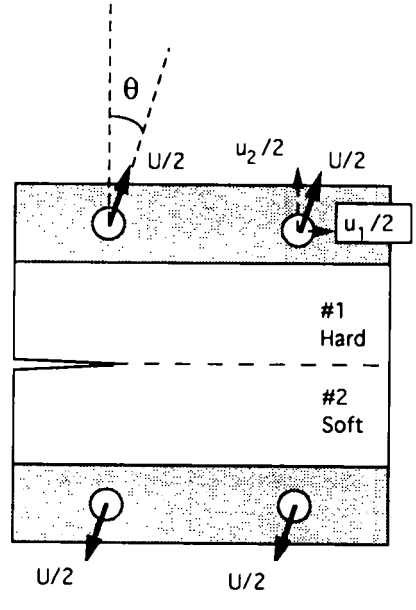

FIGURE 2 Illustration of the applied loading conditions.

Hence, an arbitrary combination of far-field tension and shear loadings can be prescribed by suitable adjustment of the loading angle. The load frame capable of accommodating various applied loading angles is described in the next section.

5 EXPERIMENTAL PROCEDURE

5.1 Loading Apparatus

The load frame assembly is presented in Figure 3. The cylindrical adaptors permit the load frame to be rigidly fastened to an MTS testing machine.[21] Owing to the compliance of the fracture specimens, the entire structural assembly, which is

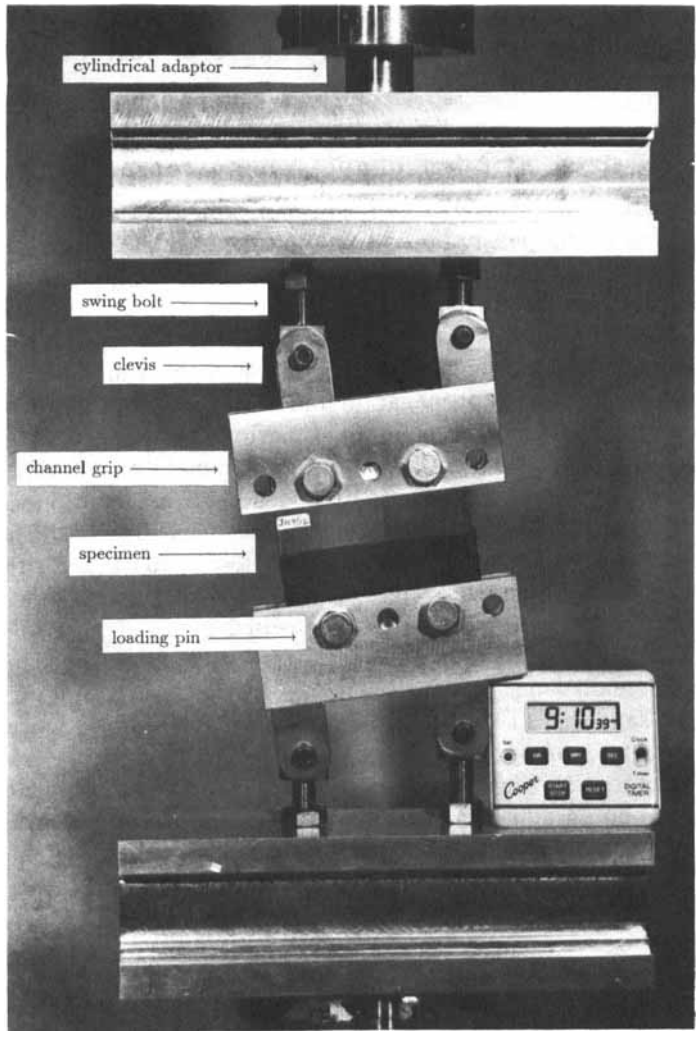

FIGURE 3 Photograph and component indentification of the loading device as mounted in the test machine.

composed of aluminum and steel, can be considered rigid. Thus, any vertical displacement imposed on the adaptors by the MTS crosshead is transmitted to the channel grips.

The orientation of the channel grips, and ultimately of the specimen, is established by adjusting the vertical and horizontal positions of the eyes of the swing bolts. The swing bolts, each with a pitch of 24 threads per inch, permit fine, incremental adjustment of vertical displacement, and hence of θ. In order to accommodate small changes in the loading angle, each channel grip is equipped with a pair of adjustable clevises. These clevises allow the grip to be rigidly fastened to the swing bolts and thus to the frame itself. The movement of each clevis is limited to the plane of the page and is confined to a 2.2 cm slot within the channel grip. This contrivance permits the grip to glide along the ray defined by the angle θ and facilitates mounting the specimen onto the load frame. Once positioned, the location of the grip relative to the clevises is held fixed with set screws.

5.2 Test Procedure

To ensure that no significant prestraining occurs as a result of affixing the specimen to the load frame, and to verify proper specimen alignment, the output of the load cell is monitored as the pins required to mount the specimen are inserted through the specimen and load frame. Refinements in specimen alignment are performed until none of the pins results in an applied load in excess of 1 N (usual load level $\sim 20N$).

For the homogeneous specimens,[22] the loading angle is maintained constant at $\theta = 0°$ in order to allow crack propagation under Mode I conditions along the interface. In contrast, a combination of far-field tension and shear loadings is required to enforce crack propagation along the interface in a bimaterial specimen. For both types of specimens, the resulting near-tip stress fields are determined by a finite element code according to the assumptions of linear elasticity. In the homogeneous case, the asymptotic fields are characterized by $K = K_I$ ($\theta = 0°$); for the bimaterial specimen, the fields are characterized by $K = (K_1^2 + K_2^2)^{1/2}$, where K_1 and K_2 represent approximately the Mode I and II stress intensities.

Crack propagation along the interface of the bimaterial specimens may be achieved for a (small) range of loading angles;[10] by trial and error it was determined that $\theta = -15.1°$ and $\theta = -19.8°$ fell within this range (at room temperature) for the bimaterial specimens analyzed here.

For each fracture test, the advancing crack is documented through periodic photo recording. The photographs are analyzed to deduce the velocity of the moving crack tip. The slope of the best-fit line through a plot of crack length *vs.* time is used to determine the crack speed.

5.3 Results and Discussion

Tests were conducted primarily at room temperature under a constant strain imposition, the magnitude of which varied from test to test. For each test, the prescribed displacements u_1, u_2 were applied suddenly at time zero and held constant there-

after. In order to identify the long-term (slow velocity) limit, some tests were performed at 60°C, and these data were combined with the room temperature data by using the time-temperature shift as estimated for the material compositions involved from Reference 13.[23]

The corresponding tests at elevated temperatures for interface data did not generate fractures which followed the interface always clearly. It did not appear proper, therefore, to include those data here; also, additional specimens from another batch were judged to have sufficiently different interface strength to make a comparison questionable.

The data summarized in Figure 4 are in the form of velocity as a function of the stress intensity factor. To construct the time-dependent Ψ functions for the two homogeneous materials, one must assemble curves of $\left[\frac{K^2/E^*}{K_o^2/E^*}\right] = \left[\frac{K}{K_o}\right]^2$ *versus* crack velocity, where K_o represents the asymptotic stress intensity factor below which crack propagation does not occur. For the two homogeneous materials, the functions Ψ are shown in Figure 5. In Figure 6, these functions have been combined according to equation (11) (*via* (7)) to construct the suggested bimaterial function Ψ_i for the interface. Here we have combined the interface data for $\theta = -15.1°$ and $-19.8°$ into a single set[24] which is seen to be best fit by Ψ_i when $K_o = 8 \times 10^{-3}$ *MPa* $m^{1/2}$ for the interface. The resulting velocity dependent fracture energy curve for the interface is then shown in Figure 7. According to this plot the intrinsic interface strength is intermediate to those of the two homogeneous solids.

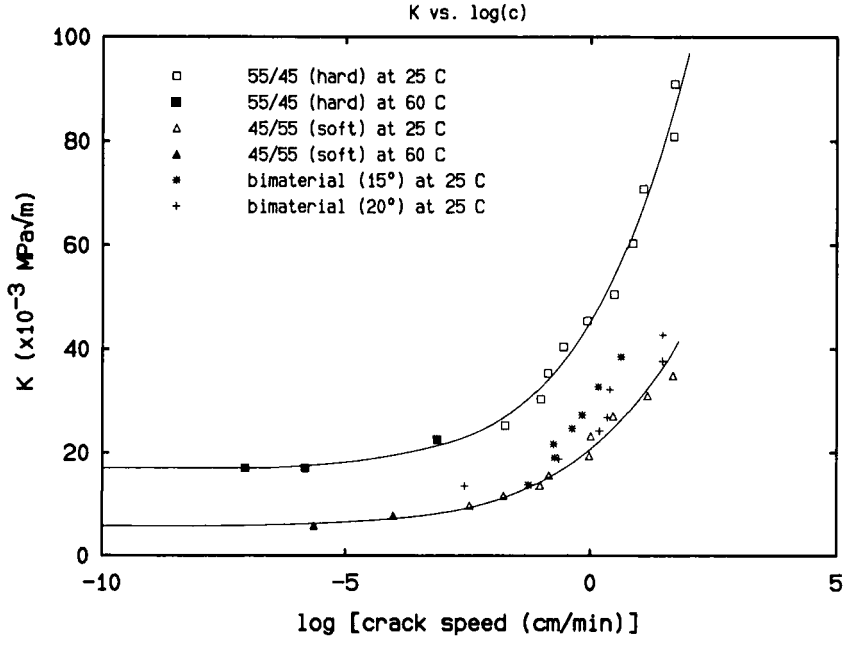

FIGURE 4 Crack propagation speed as a function of the (absolute) magnitude of stress intensity in the two adherend materials and along the bimaterial interface.

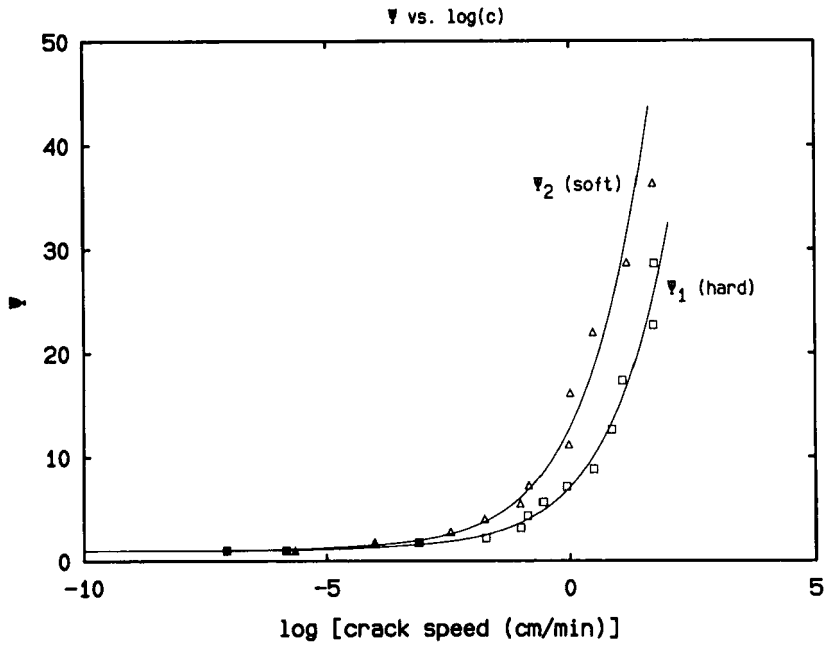

FIGURE 5 The material Ψ functions for the two solids (*cf.* equation 8).

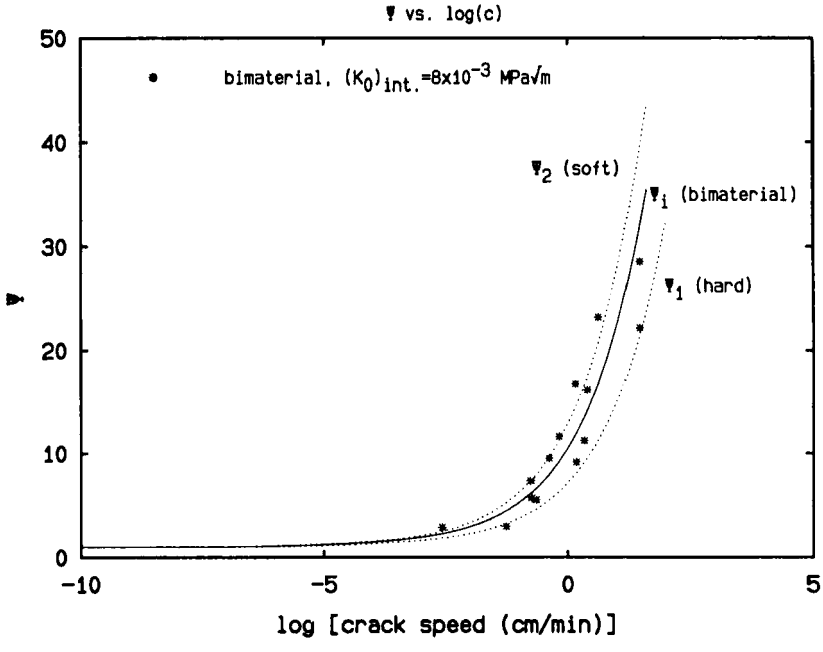

FIGURE 6 The Ψ function for bimaterial interface fracture. (Experimental points for far-field load angle θ of $-15°$ and $-20°$.)

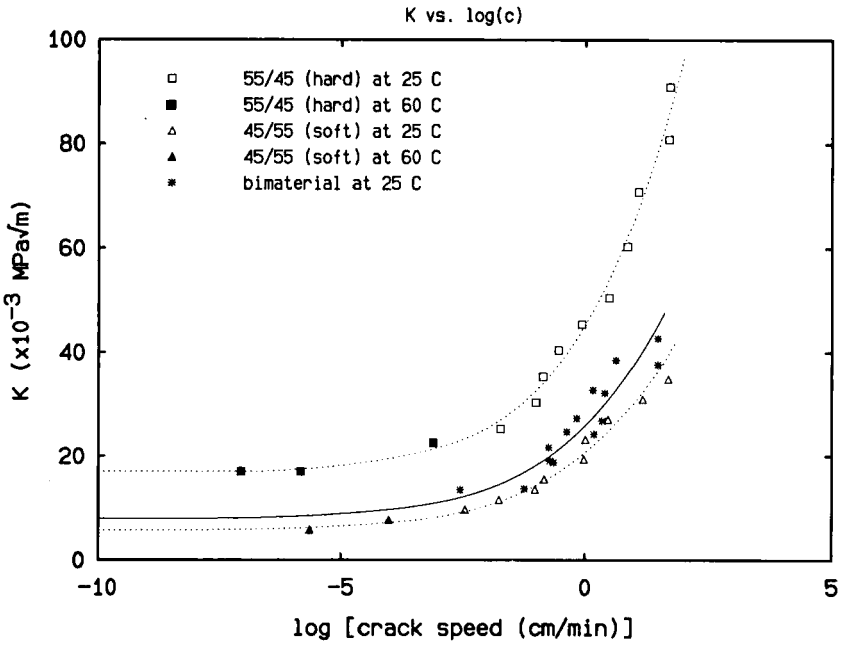

FIGURE 7 Crack propagation speed as a function of the (absolute) magnitude of the stress intensity factor; data of Figure 4 with computed curve for interfacial fracture (solid line).

6 INTERFACE STRENGTH

It becomes clear now, as pointed out in References 1 and 2, that the "interface strength" has two components: One derives from the viscoelastic contribution embodied in the function Ψ_i and the other from the intrinsic fracture energy Γ_i. Lowering the fracture energy Γ_i will shift the whole curve connecting K or $\left[\frac{K^2}{E^*}\right]$ for the interface to lower values. As a consequence, small changes in the intrinsic fracture energy may well induce rates of decohesion which differ by orders of magnitude.

As an example, consider the situation for which the "intrinsic interfacial fracture strength" has a value of only one-half of that commensurate with the interface data given in Figure 7. For comparison, the velocity dependent fracture energy curves for both the experimentally observed interface and the (hypothetically) reduced strength interface are plotted in Figure 8. To see the strong effect which the intrinsic fracture energy has on the speed of decohesion, examine the following two examples. Consider first a stress intensity imposed as indicated by the dotted line denoted by "1". The curve for the interface data indicates that the crack would propagate with a speed of $c_l = 0.17 \times 10^{-3}$ *cm/min* while the hypothetical (dashed) curve for reduced strength would allow a thousand times higher crack growth rate of $c_h = 0.17$

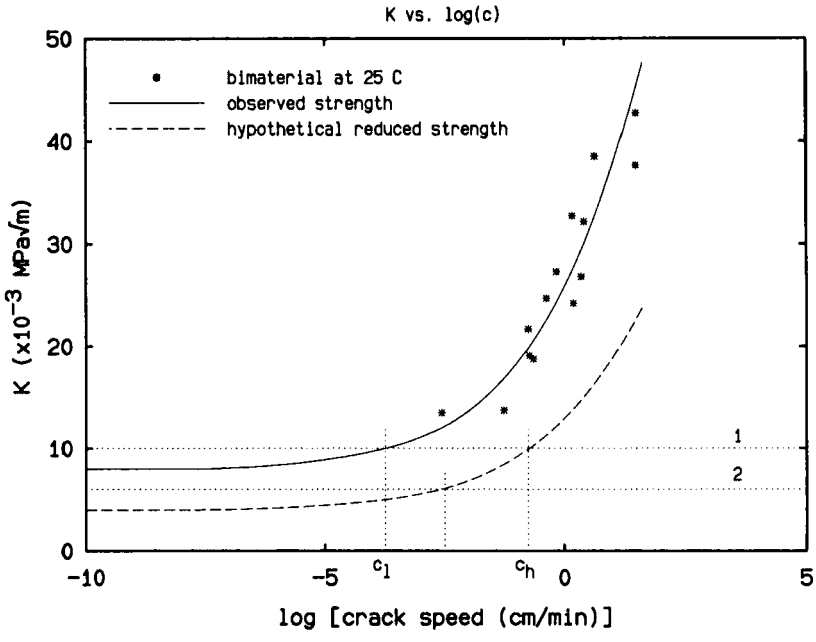

FIGURE 8 Illustration of the sensitivity of crack speed along an interface to variations in the magnitude of the intrinsic interfacial fracture energy Γ_i.

cm/min. It is clear that a relatively small change in the intrinsic fracture energy (a factor of 1/2) produces a very large velocity change.

To make the point even more explicit, consider as a second example the case for which the stress intensity factor is represented by the line denoted by "2". Since this value falls below the lowest limit of crack propagation for the interface curve, no fracture would be anticipated at all in this case, while for the case of reduced interfacial strength the crack would indeed separate the two materials at a rate of 0.30×10^{-2} *cm/min*.

6.1 A Relative Measure of Interface Strength

The above scheme of characterizing fracture strength in terms of the stress intensity or energy release rate associated with a velocity dependent function allows a quantitative characterization of a bond strength for viscoelastic materials. It is often also important to establish a measure of bond strength relative to the strength of the adherends, such as when one is interested in optimizing the former. The question arises then as to when the maximum bond strength has been achieved. Figure 7 allows a straightforward characterization of this type: We note that the intrinsic fracture energy for the interface is higher than that for the softer of the two materials. It would seem unnecessary in many situations to produce a bond strength which is higher than that of both of the two materials forming the joint. In this sense then, the bond achieved in the bimaterial specimens would seem to be optimal.

Alternately, if the observed bond strength had corresponded to the (hypothetical) curve shown dashed in Figure 8, one would conclude that less than optimal bond strength had been achieved.

This understanding is only clouded by the observation that at the elevated temperatures (60°C), the fractures did not prefer to pass strictly along the interface, but tended instead to follow into the harder of the two materials with a very small angle relative to the interface. The reason for this behavior is not necessarily a failure of the current propositions, but likely a consequence of the process in which the failure behavior was studied. The loading conditions (global loading angle) which produce crack propagation along the interface were determined by trial and error; it is visible from Figure 4 that a range of several degrees in loading angle produces some, perhaps statistically noticeable, differences at room temperature. It is well possible that the loading condition determined empirically at room temperature was less than totally satisfactory at elevated temperature when the materials respond more rapidly in fracture; in retrospect it would have been advantageous to start with the high temperature tests to determine the loading conditions more distinctly and then proceed to the lower temperatures. As it worked out, there were not enough material specimens left over to re-examine the whole test sequence, except to start with a completely new set of material castings; this is not a trivial task.

It is now of interest to return to the question regarding the magnitude of the size parameter α of the crack tip zone discussed in connection with equations (1) and (10). Recall that because of the analytical difficulties with the stress field derived from the linearized theory of (visco)elasticity, there is little hope of defining the parameter appropriate to the separation problem analytically. As stated earlier, we have assumed here that this size parameter is not very different from those for the two adherends, and that curves representing the relation between the available energy and the crack speed are similar and essentially parallel, with a shift along the ordinate in Figure 4; a sizeable difference in the α-parameter would have shown also a strong shift along the log(c) axis, with a weaker interface having the effect of shifting the data points to faster crack speeds. This reasoning would follow from equation (2), in which a lowering of the cohesive stress σ_o increases the length alpha: in order to render the same stress intensity, this increase requires that the velocity increase in a similar manner to keep α/c constant. Although there is room in the data interpretation to allow for some shifting along the ordinate or the abscissa, there is no strong indication that a pronounced shift along the abscissa has occurred or needs to be considered in the present context.

7 CONCLUSION

We have demonstrated that the time dependent unbonding of two joined viscoelastic solids follows a rate dependent fracture process which can be described to a large extent by the viscoelastic properties of the adherends; moreover, the strength of the bond can be characterized in terms of an equilibrium fracture energy, the magnitude of which characterizes the bond strength quantitatively. In addition, that interfacial and intrinsic fracture strength provides a measure of the quality of the

bond as compared with the strength of either of the two adherends, in particular with respect to the weaker of the two. While the range of viscoelastic properties represented by the materials studied is not very wide, it appears that the model of viscoelastic interface failure as proposed in an earlier work,[1] derived from essentially elastic fracture mechanics by viscoelastic analogy, has practical merit. In fact, a companion study[25] devoted to the kinking problem involved some studies at different temperatures to examine the potential effect of changing viscoelasticity on the interface fracture behavior. From those results, it appears that viscoelasticity does not significantly change the crack propagation behavior outside of the time dependence (rate effects). Thus the present results are (probably) applicable to other viscoelastic material systems, although non-linear material effects under rapid loading may also have to be considered.

Acknowledgements

The authors wish to acknowledge Air Force support under contract F04611-88-K-0024, with technical guidance provided by Dr. Chi-Tsieh Liu; additional support was received from ONR Grant N00014-91-J-1427, monitored by Dr. Peter Schmidt. Also, the competent assistance by Mr. Eli Mazor in specimen preparation and material characterization is very much appreciated.

References and Notes

1. W. G. Knauss, *J. Composite Materials,* **5,** 176–192 (1971).
2. W. G. Knauss, *Deformation and Fracture of High Polymers,* H. H. Kausch, J. A. Hassell and R. I. Jaffee, Eds. (Plenum Press, New York, 1974), pp. 501–540.
3. For plane stress conditions, simply replace $\Gamma/(1-\nu^2)$ by Γ in equation (1); also carry out this substitution for $\Gamma/(1-\nu^2)$ in all subsequent equations containing this term.
4. W. G. Knauss and H. Dietmann, *International J. Engineering Science,* **8,** 643–656 (1970).
5. W. G. Knauss and H. K. Mueller, *J. Applied Mechanics,* **38,** Series E, 483 (1971).
6. W. G. Knauss, in *The Mechanics of Fracture,* F. Erdogan, Ed., ASME, NY, AMD Vol. 19, December 1976.
7. R. A. Schapery, *International J. Fracture,* **11,** 141, 369, 549 (1975).
8. H. W. Greensmith, (1) *J. Polym. Sci.,* **21,** 175–187 (1956); (2) *J. Appl. Polym. Sci.,* **3,** No. 8, 183–193 (1960).
9. We circumvent here a discussion of the details of the "oscillatory character" of the stress field at the tip of an interface crack, and confine ourselves to the case of (nearly) incompressible materials under plane strain conditions. Thus, Poisson's ratio, ν, should always be $\sim 1/2$.
10. P. H. Geubelle and W. G. Knauss, GALCIT SM Report 91–17, California Institute of Technology, Pasadena, California, 91125, U.S.A. Submitted to *J. Appl. Mech.*
11. G. J. Lake and A. C. Thomas, *Proc. Royal Soc. London* **300,** 108–119 (1967).
12. Solithane is manufactured by Morton Thiokol, Inc. It is synthesized by mixing a "urethane resin" (isocyanate terminated polyol) and a "catalyst" (ricinus oil) at 65°C, and then curing the resulting mixture according to a curing cycle which climaxes with a 90 minute tarry at 150°C.
13. W. G. Knauss and H. K. Mueller, *AFRPL-TR-68-125 or GALCIT SM Report 67–8,* California Institute of Technology, Pasadena, California, 91125, U.S.A.
14. E. Mazor and J. M. Bowen, *GALCIT AE-100 Report,* California Institute of Technology, Pasadena, California, 91125, U.S.A.
15. J. M. Bowen, *GALCIT SM Report 90–25,* California Institute of Technology, Pasadena, California, 91125, U.S.A.
16. The "number/number" notation is used with reference to Solithane to denote the "weight percent resin-to-curative ratio"; e.g., the 55/45 composition is 55% resin and 45% curative, by weight.
17. Although the slight color difference of the two compositions permits identification of the interface between them (each exhibits a different shade of pale amber), a blue dye (Aldrich Chemical Company, Acid Blue 25) is added to the 55/45 composition in order to define this interface more clearly.
18. Miller-Stephenson Chemical Company, TFE Release Agent/Dry Lubricant, MS-122/CO2.

19. The mesh consists of approximately 2000 four-node bilinear elements concentrically focused at the tip of the crack. The number of elements, and their distribution, was slightly varied depending on the initial length of the crack.
20. Although it is recognized that pure plane stress conditions cannot prevail throughout the entire specimen, it is customary in "thin" sheet problem formulations to make this assumption.

    It is also recognized that the plane stress problem formulation omits the out-of-plane stresses which arise wholly from the elastic modulus mismatch across the interface. However, the prevailing philosophy maintains that these stresses play a secondary role in determining crack growth behavior for problems of this class, in which the in-plane stresses dominate. Inasmuch as this research constitutes an initial study of interfacial crack growth behavior, it seems reasonable to follow, at least preliminarily, this line of reasoning. Thus, the influence of these out-of-plane stresses shall not be considered here. Also, the truly three-dimensional stress field at the crack tip is thus simplified. See also Reference 10.
21. Axial-torsional load unit model number 358.10; actuator model number 358.10; transducer model number 11019 with the following load limits: axial: 3300 lb, torsional: 1500 in-lb.
22. "Homogeneous" specimens are prepared in a two-step casting procedure which is exactly analogous to the method used to manufacture bimaterial specimens as outlined in section 3.
23. The long-term modulus of Solithane 55/45 at 60°C is 3.44 *MPa*; for Solithane 45/55, it is 1.20 *MPa*.
24. The data do not seem to warrant more differentiation.
25. J. M. Bowen and W. G. Knauss, *GALCIT SM Report 91-15,* California Institute of Technology, Pasadena, California, 91125 U.S.A. Submitted to *Experimental Mechanics*.